Available online at www.sciencedirect.com
SCIENCE DIRECT®
International Journal of Heat and Mass Transfer 47 (2004) 4795–4805
International Journal of HEAT and MASS TRANSFER
www.elsevier.com/locate/ijhmt

Forced convection heat transfer from a circular cylinder in crossflow to air and liquids

S. Sanitjai, R.J. Goldstein *

Department of Mechanical Engineering, University of Minnesota, Heat Transfer Laboratory, 125, Mechanical Eng. Building, 111 Church Street SE, Minneapolis, MN 55455, USA

Received 30 July 2003; received in revised form 12 May 2004

Abstract

Local and average heat transfer by forced convection from a circular cylinder is studied for Reynolds number from 2×10^3 to 9×10^4 and Prandtl number from 0.7 to 176. For subcritical flow, the local heat transfer measurement indicates three regions of flow around the cylinder: laminar boundary layer region, reattachment of shear layer region and periodic vortex flow region. The average heat transfer in each region is calculated and correlated with the Reynolds number and the Prandtl number. The Nusselt number in each region strongly depends on the Reynolds number and the Prandtl number with different power indices. An empirical correlation for predicting the overall heat transfer from the cylinder is developed from the contributions of heat transfer in these three regions.
© 2004 Elsevier Ltd. All rights reserved.

Keywords: Heat transfer; Circular cylinder; Reynolds number; Prandtl number

1. Introduction

Though there is considerable information on the local heat transfer distribution on a circular cylinder in crossflow of air, understanding of the influence of Reynolds number (Re) and Prandtl number (Pr) on such heat transfer with different fluids is still poor, especially on the rear part of a cylinder. Using data obtained from overall (average) heat transfer measurements, previous studies have proposed empirical correlations for the overall heat transfer. However, these correlations suffer from a lack of information on the dependence on Prandtl number, and the effects of transition in the free shear layer and the wake, and significant scatter in many sets of data used for correlation. Most correlations assume that the effects of Prandtl number on the front and rear parts of the cylinder are the same with a constant power index of Prandtl number $Pr^{0.3}$ to $Pr^{0.4}$. Due to the paucity of experimental local heat transfer data over a large range of Reynolds and Prandtl numbers, the separate contributions of heat transfer on the front part and the rear part of the cylinder cannot be interpreted from previous correlations. Though a few attempts have been made to develop a correlation which shows the separate contributions of heat transfer on the front and rear parts, there are few experimental data to support the correlations since most of the previous data were obtained from overall heat transfer measurements. Till now there is essentially no correlation developed from local heat transfer data. In this paper we develop a correlation based on our local heat transfer measurements for $2\times10^3 < Re < 9\times10^4$ and $0.7 < Pr < 176$. The overall heat transfer in terms of Nusselt number (Nu) around a circular cylinder is typically correlated by a power law relationship:

$$\overline{Nu} = C \cdot Re^m \cdot Pr^n \tag{1}$$

Neglecting effects of other parameters (e.g. free stream turbulence, tunnel blockage, thermal boundary condition, and surface roughness), this correlation assumes that the Nusselt number is proportional to Re to the

* Corresponding author. Tel.: +1-612-625-5552; fax: +1-612-625-3434.
E-mail address: rjg@me.umn.edu (R.J. Goldstein).

0017-9310/$ - see front matter © 2004 Elsevier Ltd. All rights reserved.
doi:10.1016/j.ijheatmasstransfer.2004.05.012

Nomenclature

C	constant, Eq. (1)
c_{p_b}	specific heat evaluated at T_b, J/(kg K)
c_{p_f}	specific heat evaluated at T_f, J/(kg K)
c_{p_w}	specific heat evaluated at T_w, J/(kg K)
d	diameter of the circular cylinder (28.55 mm in air study)
H	height of the wind tunnel test section, (200 mm in air study)
h	local convective heat transfer coefficient, W/(m^2 K)
$\overline{h}$	average convective heat transfer coefficient, W/(m^2 K)
I	electric current, A
k_b	thermal conductivity of fluid at T_b, W/(m K)
k_f	thermal conductivity of fluid at T_f, W/(m K)
k_w	thermal conductivity of fluid at T_w, W/(m K)
L	length of heated section of test cylinder, (108 mm in air study)
Lf	length of formation region
Lt	length of transition
L_h	axial distance for voltage drop measurement, (64 mm in air study)
m	power index of Reynolds number, Eq. (1)
Nu	Nusselt number, $Nu = \frac{hd}{k_f}$
$\overline{Nu}$	average Nusselt number for $0° \leqslant \theta \leqslant 180°$, $\overline{Nu} = \frac{\overline{h}d}{k_f}$
Nu_0	Nusselt number at front stagnation point
$Nu_{0–85}$	average Nusselt number for $0° \leqslant \theta \leqslant 85°$
$Nu_{85–135}$	average Nusselt number for $85° \leqslant \theta \leqslant 135°$
$Nu_{85–180}$	average Nusselt number for $85° \leqslant \theta \leqslant 180°$
$Nu_{135–180}$	average Nusselt number for $135° \leqslant \theta \leqslant 180°$
n	power index of Prandtl number, Eq. (1)
Pr	Prandtl number, $Pr = \frac{\mu_f c_{p_f}}{k_f}$
Pr_b	Prandtl number, $Pr_b = \frac{\mu_b c_{p_b}}{k_b}$
Pr_w	Prandtl number, $Pr_w = \frac{\mu_w c_{p_w}}{k_w}$
$\dot{q}_{cd}$	conduction heat flux per unit external surface area of heater, W/m^2
$\dot{q}_{cv}$	convective heat flux per unit external surface area of heater, W/m^2
$\dot{q}_{gen}$	energy dissipation per unit external surface area of heater, W/m^2
$\dot{q}_{rd}$	radiation heat flux per unit external surface area of heater, W/m^2
r	recovery factor, Eq. (3)
Re	Reynolds number, $Re = \frac{\rho_f U d}{\mu_f}$
T_{aw}	adiabatic wall temperature, K
T_b	bulk temperature, K
T_d	dynamic temperature, K
T_f	film temperature, $T_f = 0.5(T_\infty + T_w)$, K
T_t	total temperature at the entrance of the wind tunnel, K
T_w	wall temperature, K
T_∞	free stream temperature, K
Tu	free stream turbulence intensity
ΔT	temperature difference between T_w and T_∞
U	average velocity, m/s
V	voltage drop across heater, Volt
W	width of the wind tunnel test section, (120 mm in this study)

Greek symbols

ϵ	thermal emissivity of heater surface
θ	angle around the circular cylinder, $\theta = 0°$ at front stagnation line
μ_b	dynamic viscosity evaluated at T_b, kg/(m s)
μ_f	dynamic viscosity evaluated at T_f, kg/(m s)
μ_w	dynamic viscosity evaluated at T_w, kg/(m s)
ρ_f	density evaluated at T_f, kg/m^3
σ	Stefan–Boltzmann constant, W/(m^2 K^4)

power of m and Pr to the power of n. Since flow characteristics and heat transfer mechanisms vary along the circumference of the circular cylinder, it can be expected that if a power law relation is assumed, m and n on the front and rear part of the cylinder may be different. Though a few studies were conducted to study the effects of Re and Pr, the power indices of Re and Pr have not been systematically reported.

Most early studies were concerned with overall heat transfer to different fluids. The overall convective heat transfer from smooth circular cylinders was reviewed in [1,2].

In an early study, Davis [3] measured heat transfer from wires to water, liquid paraffin, and three different transformer oils over the range of $0.14 < Re < 170$ and $3 < Pr < 1.5 \times 10^3$. The wires were electrically heated, and heat loss to the fluids was measured. It was found that heat transfer is strongly affected by the fluid properties. Additionally, a higher heat transfer rate was observed with a larger temperature difference between wall temperature and free stream temperature (ΔT). Kramers [4] correlated Davis' data for liquids and those of several investigators in air and proposed a correlation, Eq. (20) in Table 1.

Since Davis' results were limited to the low Re range, and free convection may have caused errors, Perkins and Leppert [5] conducted a study on the overall heat transfer from a circular cylinder to water and ethylene

Table 1
Empirical correlation of the overall heat transfer

Author	Correlation		Range of Re	Range of Pr
Kramers [4]	$Nu = 0.42Pr^{0.20} + 0.57Re^{0.50}Pr^{0.31}$	(20)	5–10^3	–
Perkins and Leppert [5]	$Nu\left[\frac{\mu_w}{\mu_b}\right]^{0.25} = [0.3Re^{0.5} + 0.1Re^{0.67}]Pr^{0.4}$	(21)	40–10^5	1–300
Fand [6]	$Nu_f = (0.35 + 0.34 \cdot Re_f^{0.5} + 0.15 \cdot Re_f^{0.58}) \cdot Pr_f^{0.3}$	(22)	0.1–10^5	–
Perkins and Leppert [7]	$Nu\left[\frac{\mu_w}{\mu_b}\right]^{0.25} = [0.31Re^{0.5} + 0.11Re^{0.67}]Pr^{0.4}$	(23)	40–10^5	1–300
Zukauskas and Ziugzda [8]	$Nu\left[\frac{Pr_w}{Pr_b}\right]^{0.25} = 0.26Re^{0.6}Pr^{0.37}$	(24)	10^3–2×10^5	–
Whitaker [9]	$Nu = (0.4Re^{0.5} + 0.06Re^{2/3})Pr^{0.4}\left[\frac{\mu_f}{\mu_w}\right]^{0.25}$	(25)	1–10^5	0.67–300
Churchill and Bernstein [10]	$Nu = 0.3 + \frac{0.62Re^{1/2}Pr^{1/3}}{[1+(0.4/Pr)^{2/3}]^{1/4}} \times \left[1 + \left(\frac{Re}{282,000}\right)\right]^{4/5}$	(26)	10^2–10^7	$Re \cdot Pr > 0.2$
Present correlation	$Nu = 0.446Re^{0.5}Pr^{0.35} + 0.528((6.5e^{Re/5000})^{-5} + (0.031Re^{0.8})^{-5})^{-1/5}Pr^{0.42}$	(27)	2×10^3–10^5	0.7–176

glycol covering $40 < Re < 10^5$, $1 < Pr < 300$ and $2.5 < \Delta T < 60$ °C. With a thermal boundary condition of uniform heat flux, an empirical correlation (Eq. (21) in Table 1) was proposed. Heat transfer results on the front and rear part of the cylinder were treated separately. The heat transfer contribution from the region, where the laminar boundary layer exists, is represented by the term including $Re^{0.5}$. In the rear where a periodic vortex exists, the heat transfer contribution is represented by the term including $Re^{0.67}$. Note, $Pr^{0.4}$ is used for both regions.

Fand [6] measured the overall heat transfer with a thermal boundary condition of uniform wall temperature in water covering $10^4 < Re < 10^5$ and the $2 < \Delta T < 6$ °C. A correlation was proposed, Eq. (22) in Table 1. All fluid properties were determined at the film temperature.

Even though Eqs. (21) and (22) in Table 1 appear to consider the separate contributions of heat transfer on the front part and the rear part to the overall heat transfer, there was no experimental data to support the predictions, i.e. they used total heat transfer data. Fand [6] reported the correlation of Perkins and Leppert, Eq. (21), which predicts overall Nusselt numbers 60% higher than that predicted by his correlation, Eq. (22). He gave some reasons for such a large difference. However, this difference may be caused by a treatment of Pr term, $Pr^{0.4}$ is used in Perkins and Leppert's correlation while $Pr^{0.3}$ is used in Fand's correlation.

An early study of local heat transfer from a cylinder in water was conducted by Perkins and Leppert [7]. With a uniform heat flux boundary condition, the experiments were conducted with water over the range of $2 \times 10^3 < Re < 1.2 \times 10^5$, $1 < Pr < 7$, $10 < \Delta T < 65$ °C and $0.208 < d/W < 0.415$. The effects of variation of fluid properties with ΔT were measured. They reported that the variation of fluid properties could be corrected using the factor of $(\mu_w/\mu_b)^{0.25}$. Unfortunately, they did not provide information on the separate contributions of heat transfer on the front and rear part of the cylinder. With correction for blockage based on the measured pressure distribution, they proposed a correlation, Eq. (23) in Table 1, as a modification of Eq. (21).

Zukauskas and Ziugzda [8] published a study on heat transfer from a circular cylinder in air, water, and transformer oil. The effects of Re and Pr on both local and average heat transfer were reported. For the variation of fluid properties in the boundary layer, they used the factor $(Pr_b/Pr_w)^{0.25}$ to account for the influence of sharp changes in the fluid properties.

Many other researchers proposed correlations for the overall heat transfer from a circular cylinder. Correlations, Eqs. (24)–(26) of [8–10], respectively, are given in Table 1. However, the power indices of Re and Pr for the overall heat transfer are different due to limited experimental results and significant differences in the experimental conditions of previous studies such as the ranges

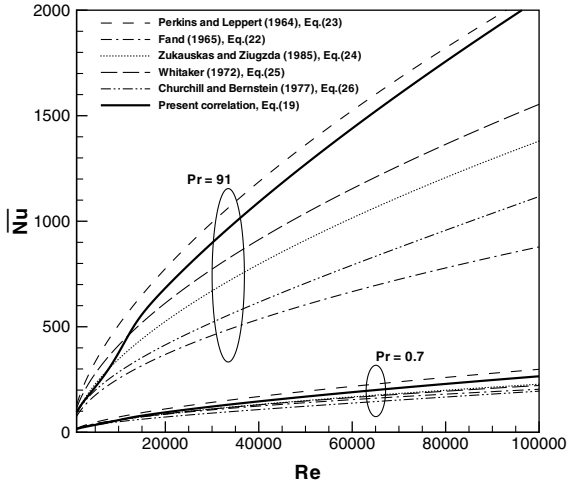

Fig. 1. Comparison of average Nusselt number predicted by various empirical correlations.

of Reynolds number and Prandtl number, and the thermal boundary condition and blockage ratio.

The Nusselt numbers calculated from the correlations in Table 1 for $Pr = 0.7$ and $Pr = 91$ are shown in Fig. 1. Note that this is in a sense an unfair comparison as not all of these correlations were derived from data over these ranges of Pr and Re. However if a single correlation is derived over a significant range of Re and Pr one must consider extrapolation using the correlation provided. For $Pr = 91$, Nusselt numbers predicted by Whitaker's correlation and Perkins and Leppert's correlation are about 50% and 100%, respectively, higher than those predicted by Churchill and Bernstein's correlation.

The objective of the present study is to determine the average heat transfer from the measured local heat transfer rates and develop an empirical equation based on the flow and heat transfer regions around the cylinder. This study provides an understanding of the effects of Re and Pr on heat transfer in different regions around the cylinder. A new empirical correlation provides accurate prediction of heat transfer coefficient, and it can be applied to a wide variety of fluids in heat transfer applications. In addition, the study provides a database for numerical predictions.

2. Experimental apparatus and instrumentation

The experiments were conducted in air, water and six mixtures of ethylene glycol and water. The range of Re is from 2×10^3 to 10^5 and a range of Pr is from 0.7 to 176. There are two tunnels used in this study. A wind tunnel was used for the air experiments, while a liquid tunnel, described in [11] was used for the experiments using water and mixtures of ethylene glycol and water. In this paper only the wind tunnel and its test section are described.

2.1. Wind tunnel

The wind tunnel (cf. [12]) is an open circuit, suction-type tunnel. Air is drawn from the laboratory room and discharged outside of the building. The entrance section consists of a bell-mouth inlet, a flow straightener and filter, three turbulence-reducing screens, and two stages of contraction (with 15:1 area ratio) ahead of the test section.

The test section is a rectangular duct of 120 mm (width)$\times$200 mm (height) cross-section and overall length of 1350 mm. The walls are 19 mm thick Plexiglas. The test cylinder is held horizontally, 712 mm from the entrance of the test section.

The flow velocity is adjusted using the discharge damper and flow control holes around the inlet duct of the fan. The maximum velocity in the test section with no cylinder present is about 100 m/s. The velocity distribution in the test section is uniform with a free stream turbulence intensity of about 0.3%.

2.2. Test cylinder

Fig. 2 shows the 28.55 mm diameter test cylinder. It consists mainly of Styrofoam to minimize conduction loss. The blockage ratio d/W of the cylinder in the test section is 0.14 which is the same as in the liquid experiments. The external surface of the test cylinder consists of an Inconel 600 foil of 25.4 μm thickness wrapped around a phenolic tube of 1 mm wall thickness. Both Styrofoam and phenolic tube are also used for the cylinder in liquid experiments. Inconel foil is attached to the tube using double-sided adhesive of 25.4 μm thickness. Power is provided by electric current passing through copper connectors at both ends of the cylinder.

Surface temperatures are obtained from eight thermocouples installed under the heating surface. Details of the temperature measurement and data acquisition system are described in [11]. For each angle around the test cylinder, the total temperatures (T_t) and surface temperatures (T_w) are measured using T-type (copper–constantan) thermocouples.

Since the dynamic temperature in the experiment is high ($0.3 < T_d < 1.4$ °C), the local adiabatic wall temperatures (T_{aw}) around the test cylinder are measured separately. They are the temperatures that the unheated cylinder attains at steady state. Local surface temperatures of the unheated cylinder are measured and presented in terms of a recovery factor (r). The dynamic temperature (T_d) and the recovery factor are defined as:

$$T_d = \frac{U_\infty^2}{2c_{pf}} \tag{2}$$

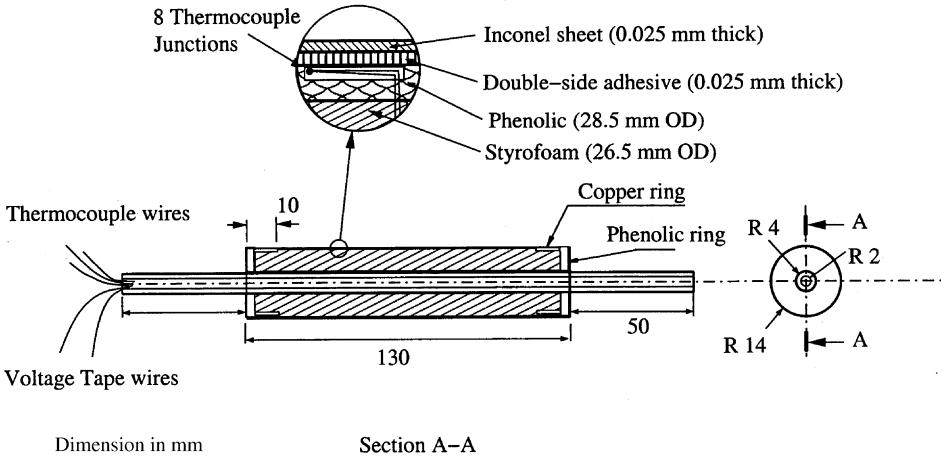

Fig. 2. Test cylinder.

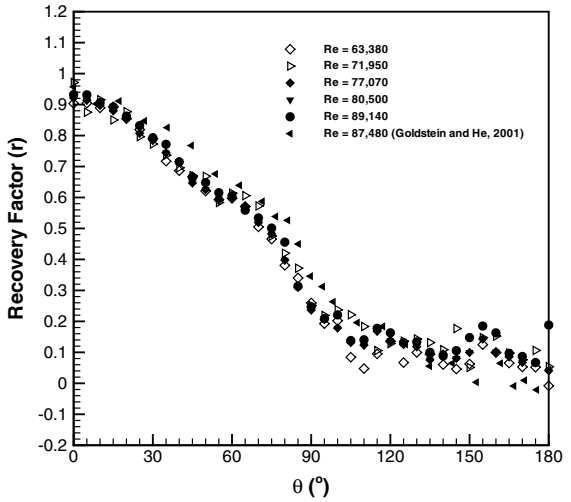

Fig. 3. Recovery factor of air around the cylinder.

$$r = 1 + \frac{T_{aw} - T_t}{T_d} \tag{3}$$

The recovery factor is shown in Fig. 3. It is close to unity at the front stagnation point of the cylinder and decreases as the flow moves downstream. Results of these measurements agree well with [12].

3. Experimental technique

The experimental technique for the tests with liquids (water and mixtures of ethylene glycol and water) is described in [11]. In this paper only the experimental technique for experiments with air is provided.

The local convective heat transfer coefficient is calculated as:

$$h = \frac{\dot{q}_{cv}}{T_w - T_{aw}} \tag{4}$$

where $\dot{q}_{cv}$ is the net convective heat transfer rate per unit area; T_w is the local surface temperature of the test cylinder and T_{aw} is the adiabatic surface temperature.

From Eq. (3), the adiabatic surface temperature is calculated as:

$$T_{aw} = T_t + (r-1)T_d \tag{5}$$

Consequently, the local heat transfer coefficient in air can be written as:

$$h = \frac{\dot{q}_{cv}}{T_w - (T_t + (r-1)T_d)} \tag{6}$$

Energy dissipated in the Inconel foil heater is transported by convection to the flow, conduction within the cylinder, and radiation to the surroundings. Thus the convective heat transfer rate per unit area ($\dot{q}_{cv}$) from the test cylinder surface is given by:

$$\dot{q}_{cv} = \dot{q}_{gen} - \dot{q}_{cd} - \dot{q}_{rd} \tag{7}$$

The energy input is determined from:

$$\dot{q}_{gen} = \frac{V \cdot I}{\pi d \cdot L_h} \tag{8}$$

where I is the electric current calculated from the voltage drop across two standard resistors, and V is the voltage drop across the axial distance L_h. Measurements indicate that is uniform over the test region.

The radiation heat loss is determined by assuming the surface of the Inconel foil to be gray with a uniform emissivity ($\epsilon = 0.1$ at 27 °C from [13]). The radiation

heat transfer rate between the test cylinder and the surroundings is determined as:

$$\dot{q}_{\mathrm{rd},\theta} = \epsilon\sigma(T_{\mathrm{w},\theta}^4 - T_\infty^4) \tag{9}$$

The maximum radiation heat loss is approximately 1.5% of $\dot{q}_{\mathrm{gen}}$ at $\theta \approx 90°$.

The 2-D heat loss by conduction from the Inconel heater to the inner core and the ends of the test cylinder is determined using the numerical program CONDUCT by Patankar [14]. The maximum conduction loss is about 7% of $\dot{q}_{\mathrm{gen}}$ at $\theta \approx 90°$ at low Re.

The uncertainty of the local heat transfer coefficient depends on the uncertainties in the temperature difference and the net convective heat loss for each test run. The experimental uncertainty evaluated based on the 95% confidence level is analyzed using the method described in [15]. The uncertainties of heat transfer coefficient and Nusselt number are 3.6% and 4.1%, respectively. The major uncertainty is from non-uniformity in temperature during the run (about 3% precision error). The uncertainties of Reynolds number and Prandtl number are 1.13% and 2.29%, respectively. The main contribution of these uncertainties is from the uncertainties of fluid properties which are conservatively estimated as: $U_\rho = \pm 0.1\%$, $U_\mu = \pm 0.5\%$, $U_{c_p} = \pm 1.0\%$, and $U_k = \pm 2.0\%$. The uncertainty in the free stream velocity is $\pm 1.0\%$.

4. Experimental results

The physical properties of the working fluids are evaluated at the film temperature (T_{f}). The local heat transfer results from a circular cylinder to liquids (water and mixtures of ethylene glycol and water) are presented in [11]. In this paper the local heat transfer to air and some ethylene glycol/water mixtures (40.7% and 81.5%) are described. Empirical correlations are also developed for the average heat transfer on the front and rear parts of the cylinder.

4.1. Local heat transfer

Figs. 4–6 show the local Nusselt number around a circular cylinder in air ($Pr = 0.7$), 40.7% mixture ($Pr \approx 22$) and 81.5% mixture ($Pr \approx 91$), respectively, at various Reynolds numbers. The Nusselt numbers are plotted versus angular distance from the front stagnation point ($\theta = 0°$) to the rear stagnation point ($\theta = 180°$). Generally, the local Nusselt number increases when the Reynolds number increases. The relatively high Nusselt numbers at the front stagnation points decline gradually with θ and reach a minimum value at $\theta \approx 85°$. For subcritical flow ($350 < Re < 2 \times 10^5$, [16]), a laminar boundary layer forms on the front of the cylinder and grows with θ. Heat transfer decreases due to the increase of thermal resistance with boundary layer growth.

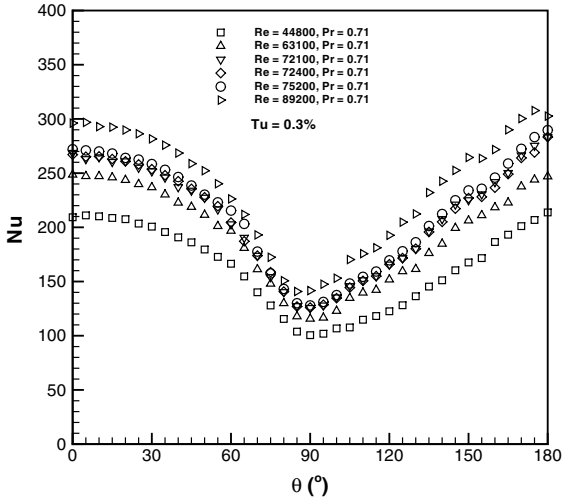

Fig. 4. Distribution of the local Nusselt number of air, $Pr = 0.7$.

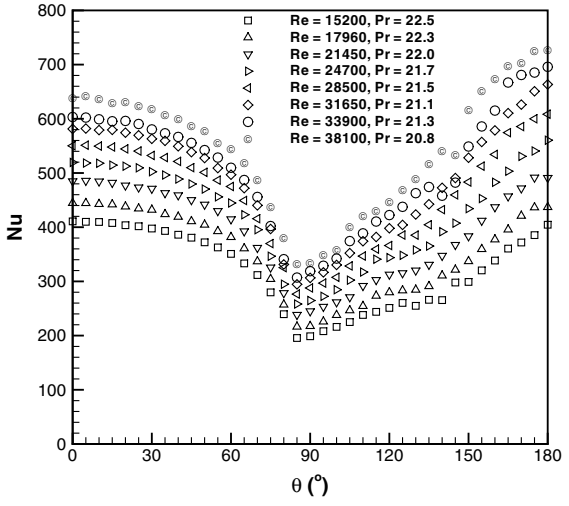

Fig. 5. Distribution of local Nusselt number at $Pr \approx 22$.

Fig. 7 shows the spread of the free shear layer and the length of formation region (Lf) and transition (Lt) from [16]. For $350 < Re < 2 \times 10^5$, Zdravkovich [16] reported that the transition occurs along the free shear layer while the boundary layer is fully laminar. For $350 < Re < 2 \times 10^3$ transition waves become visible as undulations of the free shear layers. The location of shear layer transition (Lt) is constant probably because the rate of propagation of transition in upstream direction is the same as elongation of eddies in the downstream direction. For $2 \times 10^3 < Re < 4 \times 10^4$ the transition waves

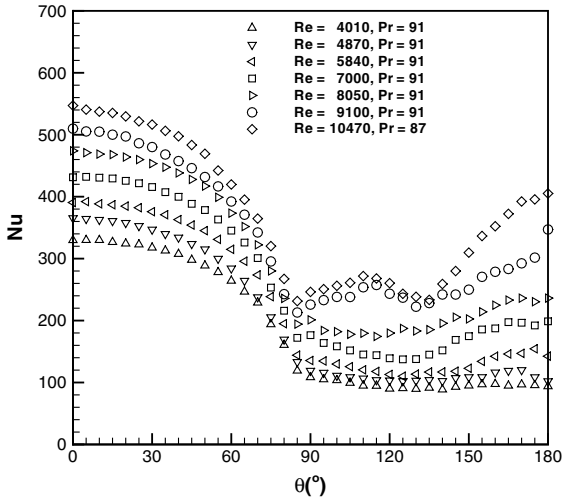

Fig. 6. Distribution of local Nusselt number at $Pr \approx 91$.

accumulate and discrete eddies along the free shear layer form and then roll up in alternating vortices. The vortex formation region moves upstream and the length of formation and transition (Lf and Lt) decreases with increasing *Re*. The periodic vortices move close to the rear surface of the cylinder. For $4 \times 10^4 < Re < 2 \times 10^5$ the free shear layer becomes turbulent. The eddy formations and turbulence bursts occur close to the separation point.

For $2 \times 10^3 < Re < 5 \times 10^3$, the results in Fig. 6 show that Nusselt number is approximately constant from $\theta = 85°$ to 180°. It is expected that the free shear layer may reattach as with laminar flow. The vortex formation region is far from the rear surface of the cylinder and the periodic vortices do not become fully turbulent. Thus, the effects of the reattached free shear layer and periodic vortices on heat transfer are relatively small.

As described in [11] and shown in Figs. 4–6, the distribution of Nusselt number around the cylinder for $5 \times 10^3 < Re < 3 \times 10^4$ can be divided into three regions, $0° < \theta < 85°$, $85° < \theta < 135°$ and $135° < \theta < 180°$. Lebouche and Martin [17] reported that, after the laminar boundary layer separation point, flow can be divided into three regions: separation bubble, reattachment of shear layer and periodic vortices in the Reynolds number range of 10^4–10^5. A hump in Nusselt number distribution in Figs. 5 and 6 between $\theta = 85°$ and 135° is caused by reattachment of the free shear layer but the flow in this region may not be fully turbulent. The Nusselt number from $\theta = 135°$ to 180° increases approximately linearly due to turbulent periodic vortices which alternately shed on both sides of the cylinder. The length of vortex formation region (Lf) decreases and the periodic vortices are located close to the rear surface for the cylinder.

Bloor [18] reported that the detached shear layer from 92° to 120° becomes turbulent for Reynolds numbers greater than 3×10^4. Thus, the reattachment of the shear layer region may become turbulent for this range of Reynolds number. For $3 \times 10^4 < Re < 9 \times 10^4$, Figs. 4 and 5 show that the Nusselt number after the minimum steadily increases and reaches a maximum at 180°

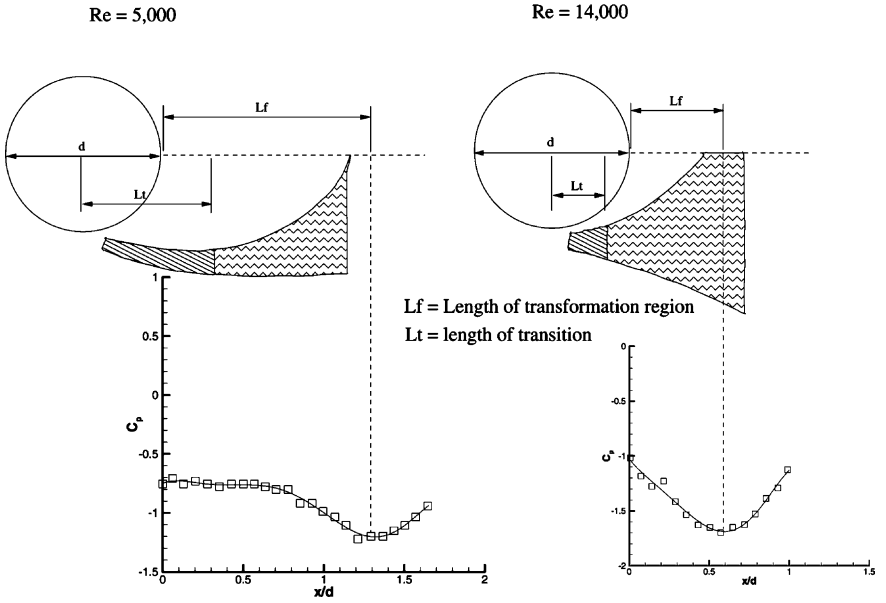

Fig. 7. Spread of free shear layer and length of formation region (Lf) and transition (Lt) adopted from [16].

because the flow in the reattached free shear layer and periodic vortex regions become fully turbulent downstream of the laminar boundary layer separation point.

4.2. Heat transfer at the front stagnation point

For $2 \times 10^3 < Re < 9 \times 10^4$ and $0.7 < Pr < 176$, the effect of the Reynolds number and the Prandtl number on the Nusselt number at the front stagnation point is shown in the lowest curve on Figs. 8 and 9, respectively. The Nusselt number can be correlated with the Reynolds number and the Prandtl number as:

$$Nu_0 = 1.11 Re^{0.5} Pr^{0.35} \tag{10}$$

Thus the power indices of Reynolds number and Prandtl number at $\theta = 0°$ are 0.5 and 0.35, respectively.

4.3. Average heat transfer results

The average heat transfer coefficient around a circular cylinder is calculated from numerical integration of the local values. For the subcritical flow region, a laminar boundary layer exists from the front stagnation point to the separation point. The Nusselt number on the front part of the cylinder from $\theta = 0°$ to 85° monotonically decreases due to growth of the laminar boundary layer. The effect of the Reynolds number and the Prandtl number on the average Nusselt number on $0° < \theta < 85°$ is shown in Figs. 8 and 9, respectively. A correlation of the average Nusselt number on this region in the form of Eq. (1) is:

$$Nu_{0\text{–}85} = 0.945 Re^{0.5} Pr^{0.35} \tag{11}$$

As might be expected over this laminar boundary layer flow region, the power indices of the Reynolds number and the Prandtl number are 0.5 and 0.35, respectively. These indices are the same as those at the front stagnation point.

As described in the local heat transfer section, the distribution of the local Nusselt number on $85° < \theta < 135°$ strongly depends on the range of the Reynolds number. An increase in the Nusselt number in this region is caused by the reattachment of the free shear layer. The effect of the Reynolds number and the Prandtl number on the average Nusselt number in this region is shown in Figs. 8 and 9, respectively. It can be observed from Fig. 8 that the average Nusselt number can be divided into two regions, i.e. $2 \times 10^3 < Re < 10^4$ and $10^4 < Re < 10^5$.

The average Nusselt number for $2 \times 10^3 < Re < 10^4$, in which the transition in the free shear layer from laminar to turbulent flow occurs and the reattached flow is not fully turbulent, can be correlated by:

$$Nu_{85\text{–}135} = 6.5 e^{Re/5000} Pr^{0.41} \tag{12}$$

The average Nusselt number for $10^4 < Re < 10^5$, in which the flow on the rear part of the cylinder is fully turbulent, can be correlated by:

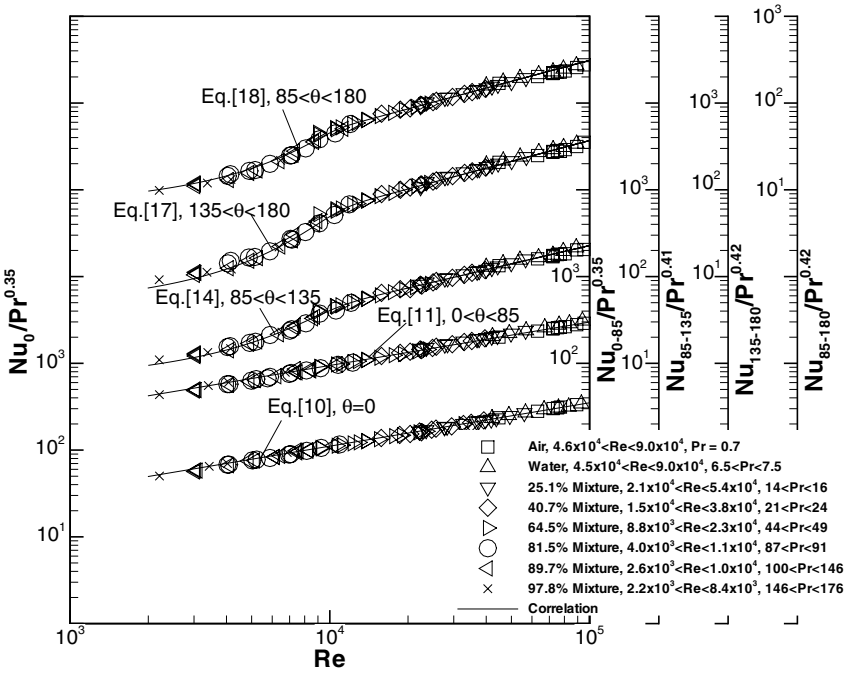

Fig. 8. Effect of Reynolds number on the average Nusselt number.

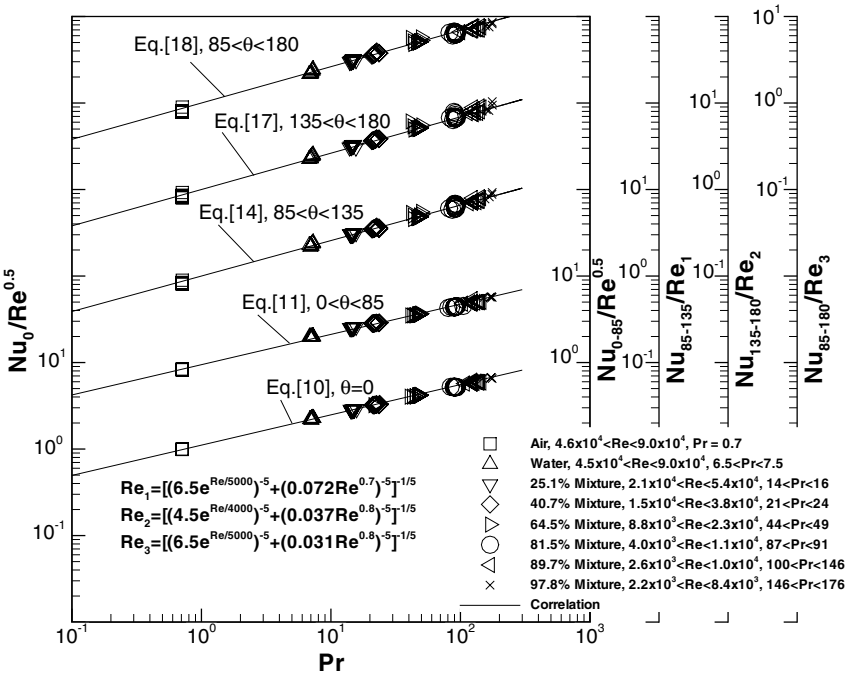

Fig. 9. Effect of Prandtl number on the average Nusselt number.

$$Nu_{85\text{–}135} = 0.072Re^{0.7}Pr^{0.41} \tag{13}$$

Thus, for $2 \times 10^3 < Re < 10^5$, $0.7 < Pr < 176$, and $85° < \theta < 135°$, as suggested in [19], the average Nusselt number can be correlated by:

$$Nu_{85\text{–}135} = ((6.5e^{Re/5000})^{-5} + (0.072Re^{0.7})^{-5})^{-1/5}Pr^{0.41} \tag{14}$$

The effect of Prandtl number on the average Nusselt number for $85° < \theta < 135°$ is shown in Fig. 9. The power index of the Prandtl number is 0.41 which is higher than that (0.35) found for the front part of the cylinder.

In the region of $135° < \theta < 180°$, an increase in the Nusselt number with θ is caused by the periodic vortex flow. The distribution of local Nusselt number depends on the range of Reynolds number. Effect of the Reynolds number and the Prandtl number on the average Nusselt number in this region is shown in Figs. 8 and 9, respectively. The data in Fig. 8 indicate that the average Nusselt number variation can again be divided into two regions, $2 \times 10^3 < Re < 10^4$ and $10^4 < Re < 10^5$.

For $2 \times 10^3 < Re < 10^4$, in which the periodic vortices are located far downstream and are not fully turbulent, the average Nusselt number can be correlated by:

$$Nu_{135\text{–}180} = 4.5e^{Re/4000}Pr^{0.42} \tag{15}$$

while for $10^4 < Re < 10^5$, when the periodic vortices are located close to the rear surface of the cylinder and are turbulent:

$$Nu_{135\text{–}180} = 0.037Re^{0.8}Pr^{0.42} \tag{16}$$

Combining these, in the range of $2 \times 10^3 < Re < 10^5$, $0.7 < Pr < 176$, and $135° < \theta < 180°$ the average Nusselt number can be correlated using:

$$Nu_{135\text{–}180} = ((4.5e^{Re/4000})^{-5} + (0.037Re^{0.8})^{-5})^{-1/5}Pr^{0.42} \tag{17}$$

The effect of Prandtl number on the average Nusselt number for $135° < \theta < 180°$ is shown in Fig. 9. The power index of the Prandtl number is 0.42 which is close to that for $85° < \theta < 135°$, but is higher than that of 0.35 on the front part of the cylinder. This indicates that the effect of the Prandtl number on the average Nusselt number on rear part of the cylinder is approximately uniform.

A correlation for average Nusselt number on the rear part of the cylinder ($85° < \theta < 180°$) for $2 \times 10^3 < Re < 10^5$, $0.7 < Pr < 176$ can be written as:

$$Nu_{85\text{–}180} = ((6.5e^{Re/5000})^{-5} + (0.031Re^{0.8})^{-5})^{-1/5}Pr^{0.42} \tag{18}$$

Effects of the Reynolds number and the Prandtl number on the average Nusselt number on $85° < \theta < 180°$ are shown in Figs. 8 and 9, respectively.

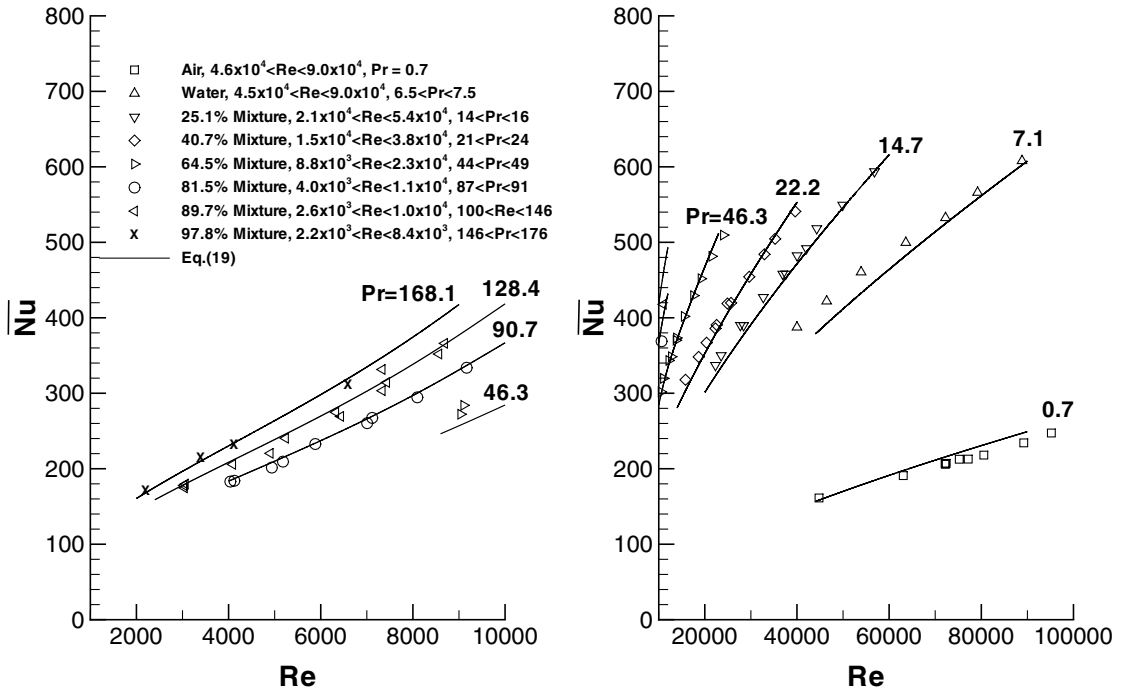

Fig. 10. Effect of Reynolds number on the overall Nusselt number around the cylinder with various fluids, $0° < \theta < 180°$.

Heat transfer results from the front and rear parts of the cylinder are treated separately. The heat transfer contribution from the region, where the laminar boundary layer exists, can be correlated with Eq. (11). In the rear part ($\theta > 85°$) where the reattachment of the free shear layer and a periodic vortex exist, the heat transfer contribution can be correlated with Eq. (18). The overall (average) Nusselt number ($0° < \theta < 180°$) is the weighted average of the Nusselt number on the front and rear parts of the cylinder and can be correlated as:

$$\overline{Nu} = 0.446Re^{0.5}Pr^{0.35} + 0.528\left(\left(6.5e^{Re/5000}\right)^{-5} + \left(0.031Re^{0.8}\right)^{-5}\right)^{-1/5}Pr^{0.42} \quad (19)$$

The effect of the Reynolds number on the overall Nusselt number for $0° < \theta < 180°$ with various Prandtl numbers is shown in Fig. 10. The solid lines in Fig. 10 show the average Nusselt number predicted by Eq. (19). The predicting lines agree well with the experimental results.

5. Comparison with earlier correlations

Fig. 11 compares the present correlation, Eq. (19), with correlations of [6–10] listed in Table 1 for the overall Nusselt number for $Pr = 0.7$ and $Pr = 91$. Experimental results for air ($Pr = 0.7$) and 81.5% mixture ($Pr \approx 91$) from the present study are also plotted and show a good agreement with the correlation, Eq. (19). The present correlation lies in the range of other correlations. The earlier correlations are generally straight lines on the log-log plot, but the current correlation has a feature which captures a transition in the range of $5 \times 10^3 < Re < 10^4$. This change occurs because of the transition of the flow in the rear part of the cylinder before becoming fully turbulent. Churchill and

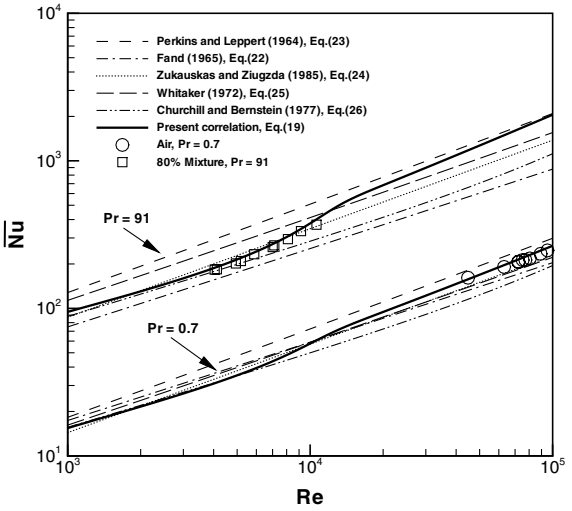

Fig. 11. Comparison of the current results and prediction with other predictions.

Bernstein [10] also observed a transition in which most of the experimental results fall higher than their prediction in this range of Reynolds number.

6. Summary and conclusions

Local heat transfer from a circular cylinder for $2 \times 10^3 < Re < 10^5$ and $0.7 < Pr < 180$ is investigated. The average heat transfer in different flow regions is obtained by numerical integration of the local heat transfer measurement in these regions. An empirical correlation for predicting heat transfer is developed for different regions on the cylinder and for the entire cylinder as well. From those results we can conclude:

1. The heat transfer variation in the range of this experimental study can be divided into three regions based on the flow structures: for $0° < \theta < 85°$, growth of the laminar boundary layer, for $85° < \theta < 135°$, reattachment of free shear layer and for $135° < \theta < 180°$, the periodic vortices.
2. Heat transfer at the front stagnation point and in the region of $0° < \theta < 85°$ is closely proportional to $Re^{0.5}$ and $Pr^{0.35}$ for constant heat flux boundary condition.
3. Heat transfer variation in the region of $85° < \theta < 135°$ depends on the range of the Reynolds number. For $5 \times 10^3 < Re < 10^4$, the average heat transfer sharply increases due to flow transition from laminar to fully turbulent. With $Re > 10^4$ heat transfer depends on $Re^{0.7}$. In this region, $Pr^{0.41}$ should be used to account for the effect of Prandtl number.
4. Heat transfer in the region $135° < \theta < 180°$ is similar to that for $85° < \theta < 135°$. With $Re > 10^4$ heat transfer is closely proportional to $Re^{0.8}$. In this region, $Pr^{0.42}$ should be used to account for the effect of Prandtl number.
5. The effect of Prandtl number on heat transfer on the front and rear parts of the cylinder is clearly illustrated. $Pr^{0.35}$ and $Pr^{0.42}$ should be used for prediction of heat transfer on the front and rear parts, respectively.
6. An empirical correlation, Eq. (19), for predicting the average heat transfer around a circular cylinder is proposed. Heat transfer in the region $85° < \theta < 135°$ and $135° < \theta < 180°$ is combined for simplicity of the correlation. This correlation demonstrates the separate contribution of heat transfer on the front and rear parts of the cylinder and is valid for $2 \times 10^3 < Re < 10^5$ and $0.7 < Pr < 176$.

Acknowledgements

Support from the Engineering Research Program of the Office of Basic Energy Science at the US Department of Energy and from the King Mongkut's University of Technology Thonburi (KMUTT) in the form of a fellowship for S. Sanitjai is gratefully acknowledged.

References

[1] A.A. Zukauskas, Heat transfer from tubes in cross-flow, Adv. Heat Transfer 8 (1972) 93–160.
[2] V.T. Morgan, The overall convective heat transfer from smooth circular cylinders, Adv. Heat Transfer 11 (1975) 199–264.
[3] A.H. Davis, Convective cooling of wires in streams of viscous liquid, Philos. Mag. 47 (1924) 1057–1092.
[4] H.A. Kramers, Heat transfer from spheres to flowing media, Physica 12 (1946) 61–80.
[5] H.C. Perkins, G. Leppert, Forced convection heat transfer from a uniformly heated cylinder, J. Heat Transfer 84 (1962) 257–263.
[6] R.M. Fand, Heat transfer by forced convection from a cylinder to water in crossflow, Int. J. Heat Mass Transfer 8 (1965) 995–1010.
[7] H.C. Perkins, G. Leppert, Local heat-transfer coefficients on a uniformly heated cylinder, Int. J. Heat Mass Transfer 7 (1964) 143–158.
[8] A. Zukauskas, J. Ziugzda, Heat Transfer of a Cylinder in Crossflow, Hemishere Pub., Washington; New York, 1985, Chapter 7.
[9] S. Whitaker, Forced convection heat transfer calculations for flow in pipes, past flat plate, single cylinder, and for flow in packed beds and tube bundles, AIChE J. 18 (1972) 361–371.
[10] S.W. Churchill, M. Bernstein, A correlating equation for forced convection from gases and liquids to a circular cylinder in cross flow, J. Heat Transfer 99 (1977) 300–306.
[11] S. Sanitjai, R.J. Goldstein, Heat transfer from a circular cylinder to mixtures of water and ethylene glycol, Int. J. Heat Mass Transfer 47 (2004).
[12] R.J. Goldstein, B. He, Energy separation and acoustic interaction in flow across a circular cylinder, J. Heat Transfer 123 (2001) 682–687.
[13] R. Siegel, J.R. Howell, Thermal Radiation Heat Transfer, third ed., Hemisphere Pub., Washington, 1992, Appendix B.
[14] S.V. Patankar, Computation of Conduction and Duct Flow Heat Transfer, Innovative Research, Maple Grove, MN, 1991.
[15] H.W. Coleman, W.G.J. Steele, Experimentation and Uncertainty Analysis for Engineers, Wiley, New York, 1989.
[16] M.M. Zdravkovich, Flow Around Circular Cylinders, Oxford University Press Inc., New York, 1997.
[17] M. Lebouche, M. Martin, Convection forcee autour du cylindre; sensibilite aux pulsations de l'ecoulement externe, Int. J. Heat Mass Transfer 18 (1975) 1161–1175.
[18] M.S. Bloor, The transition to turbulence in the wake of a circular cylinder, J. Fluid Mech. 19 (1964) 290–304.
[19] S.W. Churchill, R. Usagi, A general expression for the correlation of rates of transfer and other phenomena, AIChE J. 18 (1972) 1121–1128.